REPORT

# Mutations in *AGBL1* Cause Dominant Late-Onset Fuchs Corneal Dystrophy and Alter Protein-Protein Interaction with TCF4

S. Amer Riazuddin,[1] Shivakumar Vasanth,[2] Nicholas Katsanis,[2] and John D. Gottsch[1,*]

Fuchs corneal dystrophy (FCD) is a hereditary dystrophy of the corneal endothelium and is responsible for majority of the corneal transplantation performed in the United States. Here, we describe three generations of a family with 12 individuals affected by late-onset FCD and in which three individuals are unaffected. Genome-wide mapping provided suggestive linkage at two loci on chromosomal arms 3p and 15q. Alleles at either locus alone were not sufficient to explain FCD; however, considered together, both loci could explain the disorder in this pedigree. Subsequent next-generation sequencing identified a nonsense mutation in *AGBL1* in the 15q locus; this mutation would result in a premature termination of AGBL1. Consistent with a causal role for this transcript, further sequencing of our cohort of late-onset-FCD-affected individuals identified two cases harboring the same nonsense mutation and a further three unrelated individuals bearing a second missense allele. *AGBL1* encodes a glutamate decarboxylase previously identified in serial analysis of gene expression of corneal endothelium, a finding confirmed by immunohistochemical staining. Wild-type AGBL1 localizes predominantly to the cytoplasm; in sharp contrast, the truncated protein showed distinct nuclear localization. Finally, we show that AGBL1 interacts biochemically with the FCD-associated protein TCF4 and that the mutations found in our cohort of FCD individuals diminish this interaction. Taken together, our data identify a locus for FCD, extend the complex genetic architecture of the disorder, provide direct evidence for the involvement of TCF4 in FCD pathogenesis, and begin to explain how causal FCD mutations affect discrete biochemical complexes.

Fuchs corneal dystrophy (FCD) is the most common genetic disorder of the corneal endothelium[1–3] and accounts for a significant fraction of the corneal transplantations performed in the United States yearly.[4,5] Clinically, FCD is marked by thickening of Descemets membrane and excrescences, called guttae, that appear typically in the fourth or fifth decade.[6,7] Disease progression results in decreased visual acuity as a result of increasing corneal edema, and end-stage disease is marked by painful epithelial bullae.[8]

FCD is genetically heterogeneous. A rare early-onset form of an endothelial dystrophy with some of the clinical features of FCD has been ascribed to mutations in *COL8A2* (MIM 120252),[9,10] whereas mutations in *SLC4A11* (MIM 610206), *TCF8* (MIM 189909), and *LOXHD1* (MIM 613267) have been implicated in the pathogenesis of the common form of late-onset FCD.[9–15] Additionally, researchers have used large pedigrees that exhibit dominant inheritance with nonpenetrance and variable expressivity to map four loci, *FCD1, FCD2*, *FCD3*, and *FCD4*, on chromosomes 13, 18, 5, and 9, respectively.[13,16–18] Finally, rs613872, a common intronic SNP at the *TCF4* (MIM 602272) locus on chromosomal arm 18q has also been associated with late-onset FCD.[19–21] However haplotype analyses have suggested that this risk factor is most likely independent of *FCD2*,[21] intimating that multiple loci might account for the replicated linkage and association signals on chromosomal arm 18q.

As part of our ongoing effort to understand the genetic and molecular pathomechanisms of FCD, we recruited a large, three-generation family, DA (Figure 1). All participating individuals provided an informed written consent prior to joining the study, which was approved by the Johns Hopkins University School of Medicine Institutional Review Board (IRB) and was performed in accordance with the tenets of the Declaration of Helsinki. Overall, we were able to recruit and examine through slit-lamp biomicroscopy 16 individuals. Of these, we found 12 (nine females, three males) who fulfilled the phenotypic criteria for an FCD diagnosis (12 or more central guttae in one or in both eyes of individuals above 60 years of age). The clinical characteristics of the affected individuals of family DA present a nonuniform severity profile that typifies this disorder; some of those affected manifested a severe clinical phenotype, whereas others presented a milder phenotype (Table 1).

We first asked whether FCD in this family might be linked to any of the four reported FCD loci and/or whether affected family members might harbor mutations in the three genes causally associated with late-onset FCD. Therefore, we genotyped all available individuals with STR (short tandem repeat) microsatellite markers that span the critical intervals of *FCD1–FCD4*; both haplotype and linkage analyses ruled out these four loci (data not shown). Next, we sequenced all the coding exons along with the exon-intron boundaries of *SLC4A11*, *TCF8*, and *LOXHD1*; we did not find any causal variants

[1]The Wilmer Eye Institute, Johns Hopkins University School of Medicine, Baltimore, MD 21287, USA; [2]Center for Human Disease Modeling, Duke University, Durham, NC 27709, USA
*Correspondence: jgottsch@jhmi.edu
http://dx.doi.org/10.1016/j.ajhg.2013.08.010. 

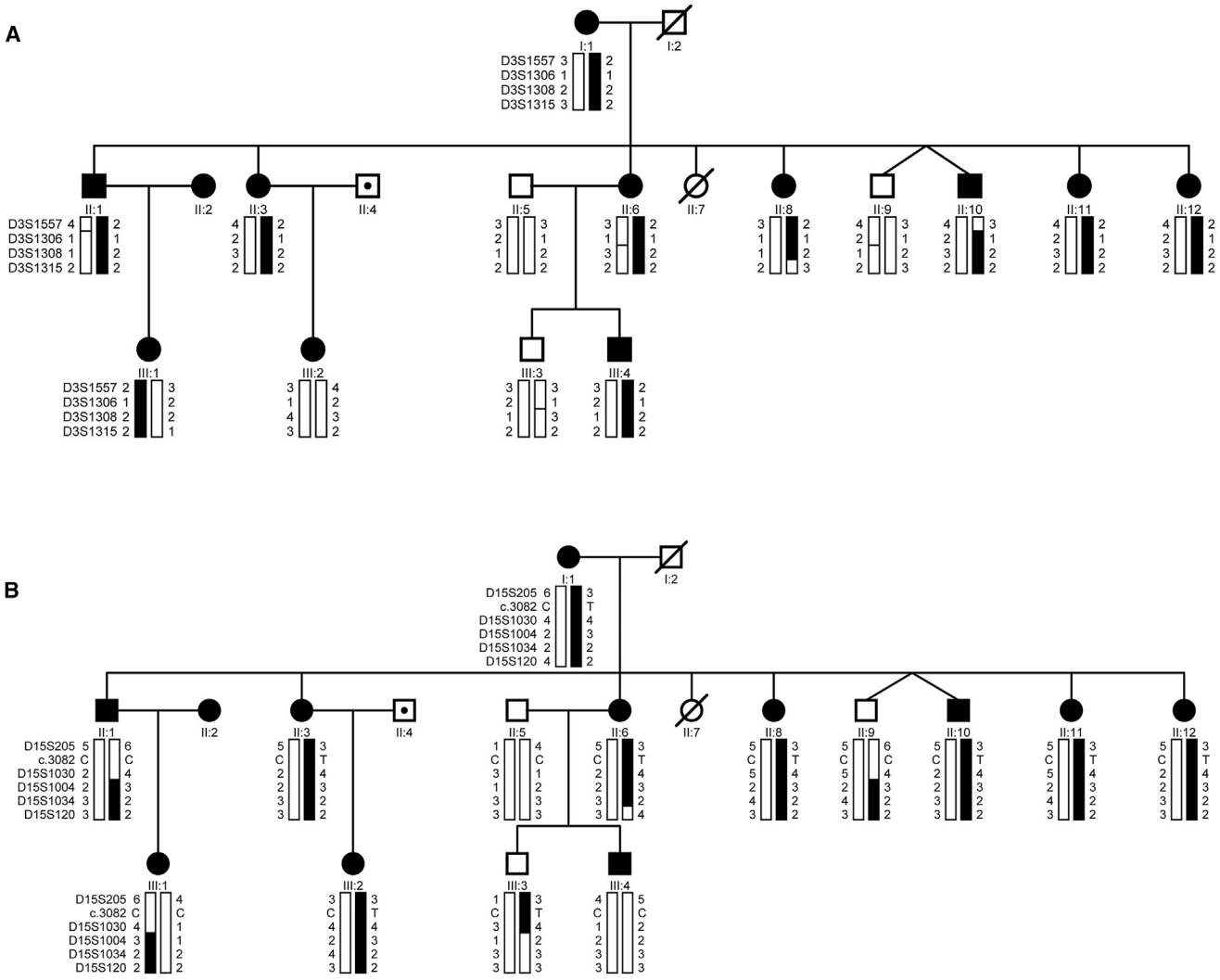


**Figure 1. Family DA Cyrillic Pedigrees Showing Haplotype, Alleles of Chromosomal Arm 3p and 15q STR Markers, and the Presence of the c.3082C>T Variant Identified in *AGBL1***

(A) Alleles forming haplotypes at chromosomal arm 3p.

(B) Alleles forming haplotypes at chromosomal arm 15q.

Filled symbol: affected individual. Diagonal line through a symbol: deceased individual. Black bars: alleles forming the disease-bearing haplotype. Note: A dot represents an individual who possesses less than 12 central guttae in one or both eyes and who therefore cannot be graded "1" on the Krachmer scale.

(data not shown). Taken together, these data are suggestive of a hitherto unknown gene or locus as the driver for FCD in this family.

To map such a locus, we performed a genome-wide two-point linkage analysis under an autosomal-dominant model with a disease allele frequency of 0.04. Initial analyses failed to detect any loci with significant LOD scores. We therefore took into consideration the nonuniform severity profile of family DA and reasoned that FCD in this family might be heterogeneous and that multiple causal alleles might be responsible for the disease phenotype, a phenomenon we have observed previously in our linkage and positional cloning studies of this disorder.[13] Thus, we recomputed linkage under a multi-locus model under the following conditions: (1) all individuals with FCD at a severity of >3.0 bilaterally on the Krachmer scale must harbor alleles at each locus; (2) individuals with FCD at a Krachmer grade $\leq$ 3.0 might harbor alleles at each locus; and (3) individuals whose parents both exhibit symptoms of FCD might not harbor alleles at any loci (the assumption was that these individuals manifest FCD as a result of a causal allele received from the parent marrying into the family DA). Even under these conditions, we did not find significant linkage; however, we did note two loci on chromosomal arms 3p and 15q; these were the only appreciable positive signals in the genome-wide scan.

To explore this finding further, we performed next-generation sequencing to pair-end sequence the exome of two affected individuals and one unaffected individual of family DA at the Cincinnati Children's Hospital and Medical Center (CCHMC) core facility. Genomic DNAs were

**Table 1. Clinical Characteristics of the Affected Individuals of Family DA**

| ID | Age (Years) | Sex | Severity | | *AGBL1* Mutation |
|---|---|---|---|---|---|
| | | | OD | OS | |
| I:1 | 89 | F | PK | PK | c.3082C>T |
| II:1 | 71 | M | 3.5 | 1.5 | wild-type |
| II:2 | 70 | F | 1.0 | 1.0 | wild-type |
| II:3 | 69 | F | 2.0 | 2.0 | c.3082C>T |
| II:4 | 65 | M | Trace | - | wild-type |
| II:6 | 69 | F | 5 | 5 | c.3082C>T |
| II:8 | 64 | F | 1.5 | 1.5 | c.3082C>T |
| II:10 | 59 | M | 2.5 | 3.0 | c.3082C>T |
| II:11 | 57 | F | 1.5 | 2.0 | c.3082C>T |
| II:12 | 55 | F | 3.5 | 3.5 | c.3082C>T |
| III:1 | 47 | F | Trace | 1.0 | wild-type |
| III:2 | 35 | F | 2.5 | 2.0 | c.3082C>T |
| III:4 | 39 | M | 1.0 | 1.25 | wild-type |

OD: oculus dexter (right eye). OS: oculus sinister (left eye). PK: penetrating keratoplasty. F: female. M: male. Penetrating keratoplasty was performed on each eye separately, and only once had the severity of disease reached 6 on the modified scale proposed by Krachmer and colleagues.[6] Note: Individual II:6 has undergone penetrating keratoplasty since the first examination.

captured with the Agilent SureSelect Human All Exon kit according to the manufacturer's instructions (Agilent). Subsequent to capture and enrichment, the paired-end library was sequenced on the Illumina HiSeq2000 Genome Analyzer (Illumina). Multiplexing of three samples per lane on a HiSeq 2000 Genome Analyzer generated $>10^8$ paired-end reads per lane. We determined that 75% of reads for each sample aligned to the reference sequence and passed quality-control filters, which was sufficient to generate on average 50× coverage for the exome, including both potential critical intervals.

The raw data were aligned to the UCSC Hg19 reference sequence by ELAND and mapped to the UCSC Hg19 reference sequence by SeqMate; SNP and INDEL (insertion/deletion) calls for each sample were made according to the GATK recommendations. The whole-exome data consisted on average of ~30,000 single-base changes and ~1,500 insertion/ deletions (indels). We examined these data by passing them through our filtering pipeline. First, we removed all the variants that were not present in either linkage interval. Subsequently, we removed all the alleles that were homozygous for the reference allele in the affected individuals. Next, we removed all variants that were heterozygous or homozygous for the alternative (nonreference) allele in the unaffected individual. Finally, we excluded all SNPs with a minor-allele frequency (MAF) > 2% in one or both affected individuals. We termed the resulting set of alleles as potential casual variants and confirmed them by dideoxy sequencing.

We identified four potential causal variants residing in the chromosome 3 region; however, none of them passed the criterion of FCD causality, suggesting (1) that this locus is an artifact and/or false-positive signal due to a miscall of alleles, (2) that the causal driver in that region does not fulfill our genetic filtering criteria, or (3) that the allele on chromosome 3 was not covered by the exome capture. In contrast, we found a C-to-T transition, c.3082C>T (Figure S1A) in ATP/GTP binding protein-like 1 (*AGBL1*; RefSeq accession number NM_152336.2), a metallocarboxypeptidase that mediates deglutamylation of target proteins residing with the putative critical interval on chromosome 15. The variant results in a premature stop codon at position 1028: p.Arg1028*. Subsequent dideoxy sequencing in the entire sibship showed that this allele segregated with an FCD haplotype in family DA (Figure 1) under the multi-locus model. Subsequently, we evaluated 384 ethnically matched controls (768 chromosomes) that had been examined thoroughly to exclude anterior segment anomalies and searched the NHLBI exome variant server database for the presence of the c.3082C>T variant. We did find this variant in two control subjects and in the NHLBI exome variant server database; however, the MAFs of 0.0026 and 0.0035 observed in control subjects and in the Northern European (Caucasian American) population, respectively, is considerably below the >4% prevalence of late-onset FCD in the US population.

To evaluate the candidacy of *AGBL1* further, we sequenced our entire FCD cohort of simplex and familial cases irrespective of known mutational burden. We identified two unrelated FCD-affected individuals who harbor the same nonsense mutation as the one found in family DA. In addition, we found a heterozygous missense variant, c.2969G>C (Figure S1B) that results in nonconserved amino acid substitution (p.Cys990Ser). The Cys at position 990 is completely conserved in all recognizable AGBL1 orthologs of the 32 species reported in the UCSC genome browser (Figure S2). This allele was absent from 384 ethnically matched controls but present in NHLBI exome variant server at a low MAF of 0.0025 in the European American population.

We noted that AGBL1 was identified previously in serial analysis of gene expression (SAGE) of human corneal endothelium (HCE).[22] To provide biological verification of that observation, we extracted HCE from postmortem eyes. We purified total RNA with Trizol (Invitrogen), and we synthesized cDNA (Invitrogen) with polydT specific primers. We then used custom Taqman probes to perform quantitative RT-PCR in triplicatewith an Applied Biosystems 7900HT system. Results were analyzed with sequence-detection software (Applied Biosystems). We recorded the mean threshold cycle (CT) value for each target (*AGBL1*) and endogenous reference (β-actin); this value represents the PCR cycle at which the ABI 7900HT detection system first detects a noticeable increase in reporter florescence above the baseline signal. We were able to detect expression of *AGBL1* in HCE at low levels

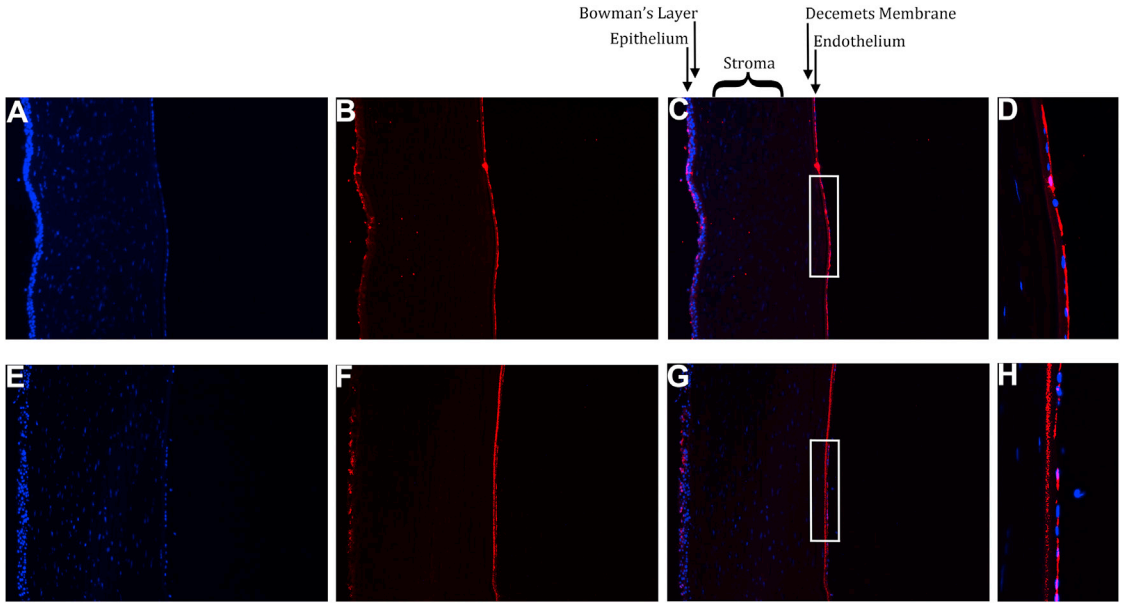


**Figure 2. Immunohistochemical Analyses of AGBL1 in 10 μm Cryosections of Human Cornea from a Patient Who Had Undergone Corneal Transplantation**

For examination of AGBL1 expression in corneal endothelium, cornea sections were stained with (A) DAPI and (B) AGBL1 antibody, whereas control slides were stained only with (E) DAPI and (F) the secondary antibody. (C and G) Merged view of images shown in (A) and (B) and in (D) and (E), respectively. (D and H) Enlarged images of boxed areas in (C) and (G).

(data not shown), confirming the expression of *AGBL1* in corneal endothelial cells.

In parallel, we evaluated the presence of AGBL1 in a human corneal section of a patient who had undergone corneal transplantation. Corneal tissue was fixed with formaldehyde and embedded in paraffin; 12-μm-thick sections were treated with rabbit polyclonal anti-ABGL1 antibody (Sigma-Aldrich) at 1:250 dilution for 4 hr at room temperature or overnight at 4°C, then with anti-rabbit IgG conjugated with AlexaFluor 594 at a 1:400 dilution (Jackson Immuno Research). Slides were costained for nuclei with DAPI (4′, 6-diamidino-2-phenylindole) at a 1:10,000 dilution(Sigma-Aldrich). Control slides were only stained with anti-rabbit IgG conjugated with AlexaFluor 594 and DAPI. Sectioned images were captured with a Zeiss-Axioskop2 microscope (Carl Zeiss Microscopy) and digitalized with ImagePro plus software, which showed distinct staining in the corneal endothelium (Figure 2).

Next, to examine the localization pattern of wild-type and mutant AGBL1, we obtained a commercially available *AGBL1* cDNA (GeneCopoeia, Rockville MD) and cloned into a 3X-Flag-tagged vector (3XFlag-pCMV10, Sigma) by amplifying the wild-type cDNA and ligating with vector by In-Fusion cloning (Clontech) as per the manufacturer's protocol. Both the missense and nonsense mutations were constructed with the QuikChange II XL Site-Directed Mutagenesis Kit (Agilent). NIH 3T3 cells were grown on cover glass pretreated with poly-L-lysine and were transfected with 1.5 μg of wild-type and mutant AGBL1 Flag-tagged constructs and Lipofectamine 2000 (Invitrogen). Cells were fixed 24 hr after transfection in 4% PFA, permeabilized, and blocked in 0.1% Triton X-100 and 1% BSA in PBS. Cells were incubated with primary and secondary antibodies at room temperature for 1 hr in blocking buffer, treated with DAPI, and mounted with VectaShield (Vector Laboratories) mounting medium. As shown in Figure 3 and Figure S3, the wild-type and the missense mutant localized to the cytoplasm. In sharp contrast, the mutant protein lacking 38 amino acids from the C terminus localized predominantly to the nucleus ($p = 0.0001$).

Taken together, our data indicate that mutations in *AGBL1* are causal to late-onset FCD and account for approximately 1%–2% of the genetic burden of the disorder. This contribution is similar to that of *LOXHD1*, *SLC4A11*, and *TCF8* mutations. To interrogate the biological significance of these findings, we asked whether AGBL1 might participate in the same biological processes as other genes previously implicated in the pathogenesis of FCD, including the associated locus TFC4. LOXHD1 and SLC4A11 are both plasma membrane proteins; however, being a transcription factor, TCF8 is found primarily in the nucleus. We therefore decided to examine the possibility that AGBL1 can interact biochemically with TCF8 (especially because one of the AGBL1 mutants is found abundantly in the nucleus). We also included TCF4, another transcription factor, because rs613872 has been associated with late-onset FCD.

HEK293 cells were transfected with Flag-AGBL1 and tested for its interaction with either Myc-TCF4 or Myc-TCF8. Two days after transfection, cells were lysed in a Triton lysis buffer with protease inhibitor cocktail and centrifuged at 13,000 g for 30 s. Lysates were then immunoprecipitated with anti-Flag-M2-antibody-conjugated

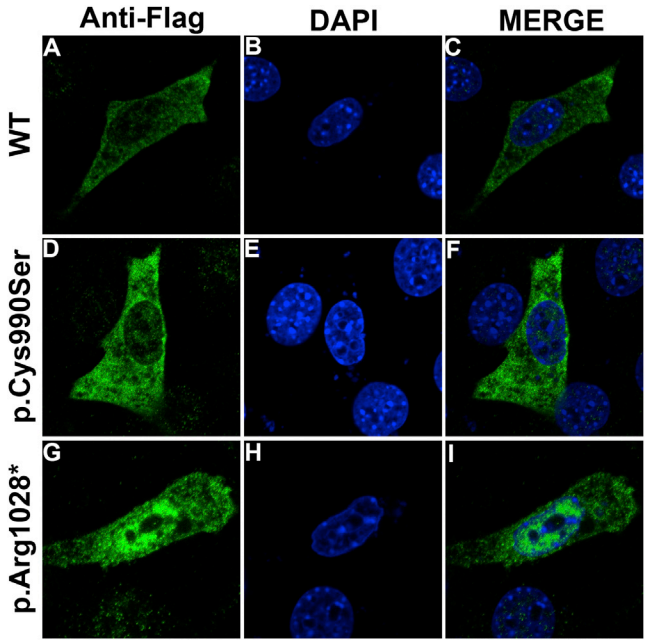


**Figure 3. The AGBL1 Nonsense Variant Is Enriched in the Nucleus**

NIH 3T3 cells were transfected with plasmids encoding Flag-tagged wild-type AGBL1 and with the two mutants, p.Cys990Ser and p.Arg1028*. Cells were stained with anti-Flag antibody (A, D, G) and DAPI (B, E and H) and co-localization was visualized by merging the two images (C, F, and I).

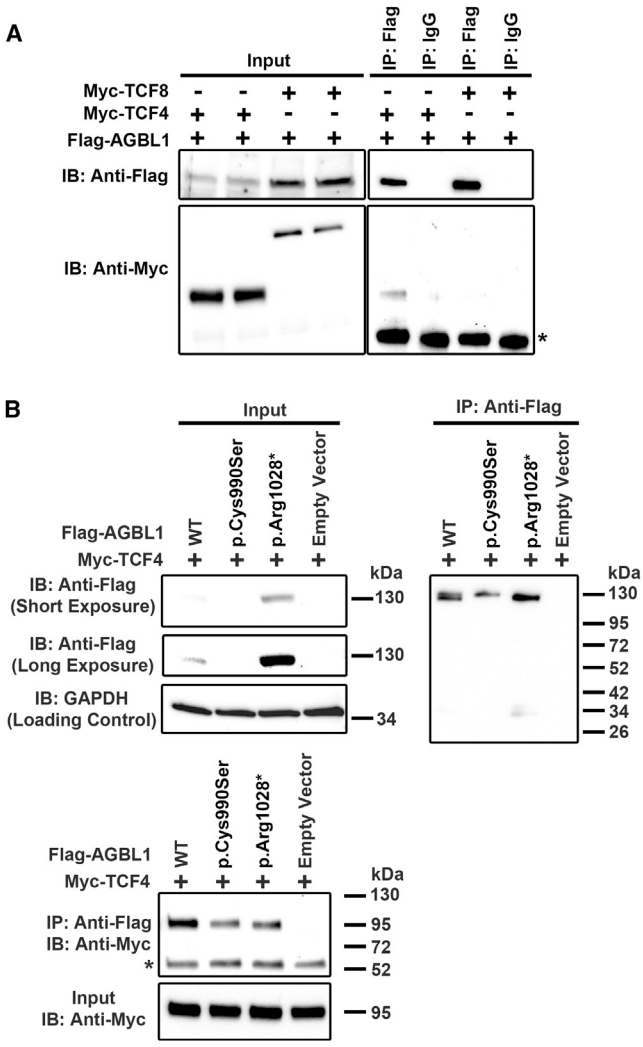


**Figure 4. AGBL1 Interacts with a Previously Identified Fuchs Locus, TCF4**

(A) HEK293 cells were transfected with Flag-AGBL1 and tested for its interaction with either Myc-TCF4 or Myc-TCF8, as shown. Immunoprecipitated lysates suggested that AGBL1 specifically interacts with TCF4 and not with TCF8.

(B) HEK293 cells were cotransfected with TCF4 and AGBL1 wild-type construct and two variants. The two AGBL1 mutants, p.Cys990Ser and pArg1028*, interact with TCF4; however, the amount of immunoprecipitated protein is diminished significantly in comparison to wild-type AGBL1, despite the higher protein amounts of mutant AGBL1.

Note: The asterisk in panels (A) and (B) indicates the heavy chain of IgG antibody that was used for immunoprecipitation.

agarose beads (Sigma), or normal mouse IgG (Santa Cruz) bound to Protein-G agarose (Santa Cruz) overnight at 4°C. Lysates were then washed three times with Triton lysis buffer. Immunoprecipitated lysates probed with anti-Myc antibody suggested that AGBL1 interacts specifically with TCF4, but not with TCF8 (Figure 4A).

The nonsense mutation in our three FCD cases is predicted to abolish the terminal 38 amino acids, whereas the missense allele was found to be a conserved residue in the other three independent FCD cases. Given the observed interaction with TCF4, we wondered whether these two variations in AGBL1 might perturb that interaction. Transfection with each of the two mutant forms of AGBL1 and wild-type TCF4 showed that the introduction of the C-terminal deletion (p.Arg1028*) significantly increases the abundance of AGBL1, whereas the p.Cys990Ser variation diminished the relative abundance of AGBL1 in comparison to the wild-type AGBL1 (Figure 4B). The difference in the relative protein levels of mutant AGBL1 strongly predicts altered stability of the mutant proteins compared to the wild-type AGBL1. Furthermore, immunoprecipitation of either of the two mutant alleles significantly reduced binding affinity to TCF4 (Figure 4B), suggesting that ablation of this interaction might contribute to disease pathogenesis.

Here we have identified *AGBL1* as a causal locus for late-onset FCD. Similar to other genes previously implicated in the pathogenesis of FCD, most notably TCF8,[13] the familial inheritance pattern of *AGBL1* is not purely Mendelian, as evidenced by the fact that three FCD in affected individuals in our index pedigree had been contributed by another locus (there was a possible signal on chromosome 3). This is not surprising, given the high frequency of the disease in the adult population and the recent documentation of both common and rare alleles, identified though a blend of association and targeted resequencing studies and affecting the causality and modification of the phenotypic expressivity of the disorder in FCD-affected individuals.[13] Despite these complexities, however, the study of large multigenerational pedigrees

remains important in the discovery of causal alleles in FCD.[13–15,18] Here, we add a glutamylase to the series of proteins that drive the disorder. The glutamylase enzyme (metallocarboxypeptidase) catalyzes the deglutamylation of polyglutamate side chains generated by posttranslational polyglutamylation in proteins.[23] It has been shown that controlling the length of the polyglutamate side chains on tubulin is critical for neuronal survival and that the lack of such control results in neurodegeneration in mice.[23]

Importantly, the observed interaction between AGBL1 and TCF4 directly intimates the latter protein in the causality of FCD (prior evidence being exclusively based on GWAS association) and provides a potential mechanism for the observed AGBL1 mutations. We speculate that TCF4 might be an enzymatic target for AGBL1. Although this result will require experimental validation, it is tempting to speculate that other targets of AGBL1 might now become natural candidates for causing FCD as well, whereas restoration of lost glutamylase activity and its consequences might be an area of potential therapeutic-target development.

## Supplemental Data

Supplemental Data include three figures and can be found with this article online at http://www.cell.com/AJHG/.

## Acknowledgments

We thank all family members for their participation in this study. None of the contributing authors have any financial interest related to this work. This study was supported in part by National Eye Institute Grant R01EY016835 and the Kwok Research Fund. J.D.G. is the Margaret C. Mosher Professor of Ophthalmology. N.K. is a Distinguished Brumley Professor.

Received: April 1, 2013
Revised: July 8, 2013
Accepted: August 13, 2013
Published: October 3, 2013

## Web Resources

The URLs for data presented herein are as follows:

Genome Analysis Toolkit, http://www.broadinstitute.org/gatk
Online Mendelian Inheritance in Man (OMIM), http://www.omim.org
UCSC Genome Browser, http://genome.ucsc.edu/

## References

1. Fuchs, E. (1910). Dystrophia epithelialis corneae. Graefes Arch Clin Exp Ophthalmol (76):478-508 2. Wilson SE and Bourne WM (1988) Fuchs' dystrophy. Cornea *7*, 2–18.
2. Wilson, S.E., and Bourne, W.M. (1988). Fuchs' dystrophy. Cornea *7*, 2–18.
3. Klintworth, G.K. (2003). The molecular genetics of the corneal dystrophies–current status. Front. Biosci. *8*, d687–d713.
4. Lorenzetti, D.W., Uotila, M.H., Parikh, N., and Kaufman, H.E. (1967). Central cornea guttata. Incidence in the general population. Am. J. Ophthalmol. *64*, 1155–1158.
5. Mannis, M.J., Holland, E.J., Beck, R.W., Belin, M.W., Goldberg, M.A., Gal, R.L., Kalajian, A.D., Kenyon, K.R., Kollman, C., Ruedy, K.J., et al. (2006). Clinical profile and early surgical complications in the Cornea Donor Study. Cornea *25*, 164–170.
6. Krachmer, J.H., Purcell, J.J., Jr., Young, C.W., and Bucher, K.D. (1978). Corneal endothelial dystrophy. A study of 64 families. Arch. Ophthalmol. *96*, 2036–2039.
7. Gottsch, J.D., Sundin, O.H., Rencs, E.V., Emmert, D.G., Stark, W.J., Cheng, C.J., and Schmidt, G.W. (2006). Analysis and documentation of progression of Fuchs corneal dystrophy with retroillumination photography. Cornea *25*, 485–489.
8. Goar, E.L. (1933). Dystrophy of the Corneal Endothelium (Cornea Guttata), with Report of a Histologic Examination. Trans. Am. Ophthalmol. Soc. *31*, 48–59.
9. Biswas, S., Munier, F.L., Yardley, J., Hart-Holden, N., Perveen, R., Cousin, P., Sutphin, J.E., Noble, B., Batterbury, M., Kielty, C., et al. (2001). Missense mutations in COL8A2, the gene encoding the alpha2 chain of type VIII collagen, cause two forms of corneal endothelial dystrophy. Hum. Mol. Genet. *10*, 2415–2423.
10. Gottsch, J.D., Sundin, O.H., Liu, S.H., Jun, A.S., Broman, K.W., Stark, W.J., Vito, E.C., Narang, A.K., Thompson, J.M., and Magovern, M. (2005). Inheritance of a novel COL8A2 mutation defines a distinct early-onset subtype of fuchs corneal dystrophy. Invest. Ophthalmol. Vis. Sci. *46*, 1934–1939.
11. Gottsch, J.D., Zhang, C., Sundin, O.H., Bell, W.R., Stark, W.J., and Green, W.R. (2005). Fuchs corneal dystrophy: aberrant collagen distribution in an L450W mutant of the COL8A2 gene. Invest. Ophthalmol. Vis. Sci. *46*, 4504–4511.
12. Vithana, E.N., Morgan, P.E., Ramprasad, V., Tan, D.T., Yong, V.H., Venkataraman, D., Venkatraman, A., Yam, G.H., Nagasamy, S., Law, R.W., et al. (2008). SLC4A11 mutations in Fuchs endothelial corneal dystrophy. Hum. Mol. Genet. *17*, 656–666.
13. Riazuddin, S.A., Zaghloul, N.A., Al-Saif, A., Davey, L., Diplas, B.H., Meadows, D.N., Eghrari, A.O., Minear, M.A., Li, Y.J., Klintworth, G.K., et al. (2010). Missense mutations in TCF8 cause late-onset Fuchs corneal dystrophy and interact with FCD4 on chromosome 9p. Am. J. Hum. Genet. *86*, 45–53.
14. Riazuddin, S.A., Vithana, E.N., Seet, L.F., Liu, Y., Al-Saif, A., Koh, L.W., Heng, Y.M., Aung, T., Meadows, D.N., Eghrari, A.O., et al. (2010). Missense mutations in the sodium borate cotransporter SLC4A11 cause late-onset Fuchs corneal dystrophy. Hum. Mutat. *31*, 1261–1268.
15. Riazuddin, S.A., Parker, D.S., McGlumphy, E.J., Oh, E.C., Iliff, B.W., Schmedt, T., Jurkunas, U., Schleif, R., Katsanis, N., and Gottsch, J.D. (2012). Mutations in LOXHD1, a recessive-deafness locus, cause dominant late-onset Fuchs corneal dystrophy. Am. J. Hum. Genet. *90*, 533–539.
16. Sundin, O.H., Jun, A.S., Broman, K.W., Liu, S.H., Sheehan, S.E., Vito, E.C., Stark, W.J., and Gottsch, J.D. (2006). Linkage of late-onset Fuchs corneal dystrophy to a novel locus at 13pTel-13q12.13. Invest. Ophthalmol. Vis. Sci. *47*, 140–145.
17. Sundin, O.H., Broman, K.W., Chang, H.H., Vito, E.C., Stark, W.J., and Gottsch, J.D. (2006). A common locus for late-onset Fuchs corneal dystrophy maps to 18q21.2-q21.32. Invest. Ophthalmol. Vis. Sci. *47*, 3919–3926.

18. Riazuddin, S.A., Eghrari, A.O., Al-Saif, A., Davey, L., Meadows, D.N., Katsanis, N., and Gottsch, J.D. (2009). Linkage of a mild late-onset phenotype of Fuchs corneal dystrophy to a novel locus at 5q33.1-q35.2. Invest. Ophthalmol. Vis. Sci. *50*, 5667–5671.
19. Baratz, K.H., Tosakulwong, N., Ryu, E., Brown, W.L., Branham, K., Chen, W., Tran, K.D., Schmid-Kubista, K.E., Heckenlively, J.R., Swaroop, A., et al. (2010). E2-2 protein and Fuchs's corneal dystrophy. N. Engl. J. Med. *363*, 1016–1024.
20. Li, Y.J., Minear, M.A., Rimmler, J., Zhao, B., Balajonda, E., Hauser, M.A., Allingham, R.R., Eghrari, A.O., Riazuddin, S.A., Katsanis, N., et al. (2011). Replication of TCF4 through association and linkage studies in late-onset Fuchs endothelial corneal dystrophy. PLoS ONE *6*, e18044.
21. Riazuddin, S.A., McGlumphy, E.J., Yeo, W.S., Wang, J., Katsanis, N., and Gottsch, J.D. (2011). Replication of the TCF4 intronic variant in late-onset Fuchs corneal dystrophy and evidence of independence from the FCD2 locus. Invest. Ophthalmol. Vis. Sci. *52*, 2825–2829.
22. Gottsch, J.D., Bowers, A.L., Margulies, E.H., Seitzman, G.D., Kim, S.W., Saha, S., Jun, A.S., Stark, W.J., and Liu, S.H. (2003). Serial analysis of gene expression in the corneal endothelium of Fuchs' dystrophy. Invest. Ophthalmol. Vis. Sci. *44*, 594–599.
23. Rogowski, K., van Dijk, J., Magiera, M.M., Bosc, C., Deloulme, J.C., Bosson, A., Peris, L., Gold, N.D., Lacroix, B., Grau, M.B., et al. (2010). A family of protein-deglutamylating enzymes associated with neurodegeneration. Cell *143*, 564–578.